Development of novel nanoporous hexagonal tungsten oxide membrane for separation of water/acetic acid mixtures *via* pervaporation

Hiroto Kunishi[a], Takeshi Hagio[a,b,*], Shintaro Wada[c], Yuki Kamimoto[a,b], Ryoichi Ichino[a,b]

[a]Department of Chemical Systems Engineering, Graduate School of Engineering, Nagoya University, Furo-cho, Chikusa-ku, Nagoya, Aichi 464-8603, Japan

[b]Institute of Materials Innovation, Institutes of Innovation for Future Society, Nagoya University, Furo-cho, Chikusa-ku, Nagoya, Aichi 464-8601, Japan

[c]Department of Materials Science and Engineering, School of Engineering, Nagoya University, Furo-cho, Chikusa-ku, Nagoya, Aichi 464-8603, Japan

*Corresponding Author: Takeshi Hagio, e-mail: hagio@mirai.nagoya-u.ac.jp, Tel: +81 52 747 6594

Others contact information

Hiroto Kunishi, e-mail: kunishi.hiroto@d.mbox.nagoya-u.ac.jp

Shintaro Wada, e-mail: wada.shintaro@d.mbox.nagoya-u.ac.jp

Yuki Kamimoto, e-mail: yuki.kamimoto@mirai.nagoya-u.ac.jp

Ryoichi Ichino, e-mail: ichino.ryoichi@material.nagoya-u.ac.jp

Abstract

A novel nanoporous hexagonal tungsten oxide (NP-h-WO_3) membrane was developed for separating water/acetic acid (H_2O/AcOH) mixtures. The nanopores on the c-plane of h-WO_3 are larger than H_2O molecules and smaller than AcOH molecules and thus should allow for their effective separation. Moreover, h-WO_3 exhibits high stability in acids (pH < 4). Therefore, c-axis-aligned NP-h-WO_3 membranes are promising for the separation of H_2O/AcOH mixtures. Given this background, we report, for the first time, the synthesis of c-plane-aligned dense NP-h-WO_3 membranes on porous ceramic supports *via* the hydrothermal method using a precursor solution containing AcOH. The presence of AcOH and the concentration of Na_2WO_4 in the precursor solution are the key factors affecting crystal growth and alignment along the c-plane. A high Na_2WO_4 concentration is necessary for obtaining membranes with a high degree of c-plane alignment. Thus, dense, c-plane-aligned NP-h-WO_3 membranes could be fabricated by precoating the support with amorphous WO_3 seeds and subsequent hydrothermal synthesis in a precursor solution of Na_2O/WO_3/AcOH/H_2O (1/1/0.88/201) at 180 °C for 24 h. The fabricated membranes exhibited a maximum separation factor of 42.6 during the pervaporation of a H_2O/AcOH mixture (10/90 (w/w)) at 80 °C. Thus, these NP-h-WO_3 membranes are highly suited for H_2O/AcOH separation.

Keywords: nanoporous hexagonal tungsten oxide, separation membrane, water/acetic acid mixture, pervaporation

1. Introduction

Currently, the dehydration of organic solvents is generally achieved through distillation, which is an energy consuming process, especially in the case of azeotropic and close-boiling-point mixtures. Pervaporation (PV) using nanoporous membranes is considered an eco-friendly separation method for such mixtures because it allows for the separation of mixtures based on the differences in the molecular sizes of the components. Conventionally, zeolite membranes have been used for this purpose, owing to their nanoporous structure and desirable thermal, mechanical, and chemical properties, which are superior to those of their organic counterparts [1]. Till now, various types of zeolites have been tested for use as membrane materials, including LTA-type zeolite [2], FAU-type zeolite [3], MOR-type zeolite [4], MFI-type zeolite [5], and CHA-type zeolite [6]. Several zeolite membranes, such as those of MOR-type, CHA-type, and MFI-type zeolites, have been found to exhibit excellent separation performances with respect to water (H_2O)/organic solvent mixtures during vapor permeation and/or PV [7-9].

Among the various organic solvents investigated, acetic acid (AcOH) is an important chemical intermediate in the synthesis of vinyl acetate, terephthalic acid, cellulose ester, and other esters [10]. However, the development of separation membranes for dehydrating H_2O/AcOH mixtures remains a significant challenge because the membrane materials must exhibit high acid resistance, and conventional membrane materials do not meet this requirement [11,12]. Therefore, the development of novel separation membranes that can resist acidic systems is necessary.

Tungsten oxide has been reported to crystallize in the form of various polymorphs, such as monoclinic, orthorhombic, hexagonal, and many other forms [13,14]. Among them, hexagonal tungsten oxide (h-WO_3) exhibits a unique nanoporous structure. It forms a hexagonal, symmetric prism consisting of a WO_6 octahedral framework and exhibits

hexagonal tunnels along the c-axis [15]. Owing to its unique structure, nanoporous h-WO_3 (NP-h-WO_3) is used in many applications and devices, such as electrochromic devices, semiconductor sensors, and photocatalysis [16]. It has been reported that the openings of these hexagonal tunnels have a diameter of 0.367 nm [17], which is larger than the diameter of the H_2O molecule (0.26 nm) and smaller than the diameter of the AcOH molecule (0.436 nm) [18]. Moreover, WO_3 is known for its high stability in acids at pH levels lower than 4 [19,20]. Therefore, dense NP-h-WO_3 membranes that exhibit c-plane alignment would be promising for use as separation membranes for the dehydration of H_2O/AcOH mixtures. However, most previous reports on the hydrothermal synthesis of NP-h-WO_3 crystals state that the crystals generally exhibit a one-dimensional (1D) whisker-like or thin, rod-like structure and have an extremely small c-plane area [21]. Further, it is difficult to form a dense c-plane-aligned film [22]. Therefore, a new method for growing dense c-plane-aligned NP-h-WO_3 membranes must be developed to fabricate the desired separation membranes.

Recently, our research group discovered that the use of a precursor solution containing AcOH for the hydrothermal synthesis of NP-h-WO_3 effectively promotes the growth of the c-plane [23]. Here, we report, for the first time, the synthesis of dense c-plane-aligned NP-h-WO_3 membranes on porous ceramic supports by the hydrothermal method using a precursor solution containing AcOH. We investigated the effects of the presence of AcOH and the concentration of sodium tungstate (Na_2WO_4) in the precursor solution as well as those of the preseeding of amorphous WO_3 on the ceramic support and the synthesis time on the crystal growth and alignment in the NP-h-WO_3 membranes. Finally, the performances of the membranes were evaluated with respect to the separation of H_2O/AcOH mixtures by PV.

2. Experimental

2.1. Materials

Handmade porous disk-like supports (diameter: ~30 mm, thickness: 1.0 mm, and porosity: ~40% or diameter: ~11 mm, thickness: ~1.5 mm, and porosity: ~35%) were prepared by sintering green bodies consist of rutile titania powder (TiO_2, Kanto Chemical Co., Inc., purity: ≥99.0%). Porous tubular ceramic supports (outer diameter: 12 mm, inner diameter: 9 mm, and porosity: ~35%) were purchased from NGK Filtech Co., Ltd. and cut into 10-mm-long pieces. Both types of supports were rinsed by sonication in water and ethanol for ~10 min each and completely dried before use.

Sodium tungstate dihydrate ($Na_2WO_4 \cdot 2H_2O$, Nacalai Tesque, Inc., purity: ≥98%), 35% hydrochloric acid (HCl, Nacalai Tesque, Inc.), and AcOH (Nacalai Tesque, Inc., purity: ≥99%) were used to prepare the precursor solution for the hydrothermal synthesis of NP-h-WO_3. AcOH was also used to prepare the H_2O/AcOH mixtures used for evaluating the separation performances of the fabricated membranes. Methanol (MeOH, Nacalai Tesque, Inc., purity: ≥99.8%), ethanol (EtOH, Nacalai Tesque, Inc., purity: ≥99.5%), acetone (Actn, Nacalai Tesque, Inc., purity: ≥99.5%), and the aforementioned AcOH were used for measuring the single component permeation. All the chemicals were used in the as-received form, except for MeOH, EtOH, Actn, which were priorly dehydrated using molecular sieves (Nacalai Tesque, Inc., Molecular Sieves 4A NRG, beads, particle size abt. 2 mm).

2.2. Synthesis of NP-h-WO_3 membranes

The precursor solution for membrane synthesis was prepared using the following procedure. First, $Na_2WO_4 \cdot 2H_2O$ was completely dissolved in distilled water. Next, either HCl or AcOH was added dropwise to the $Na_2WO_4 \cdot 2H_2O$ solution under thorough mixing until the pH reached ~2 and was further mixed for 5 min. Then, the porous supports, which were either unseeded or seeded with an amorphous WO_3 powder by dip coating (See

Supplementary Information for the method used to prepare the amorphous WO_3 seeds), were placed in Teflon containers using a Teflon holder, and 60 ml of the precursor solution was added to the containers. The Teflon containers were then sealed and placed in a stainless steel autoclave (SAN-AI Kagaku Co. Ltd., HU-100). Hydrothermal synthesis was performed at 453 K in a convection oven (AS ONE Corporation, MOV-450). After the completion of the synthesis process, the membranes were repeatedly rinsed and sonicated in distilled water and ethanol to remove both the weakly attached crystals on the membrane surface and the precursor solution remaining inside the porous support and then dried at 343 K overnight. After being dried, the membranes were stored at room temperature. The effects of the acid type, seeding, synthesis time, and precursor solution composition on the formation of the NP-h-WO_3 membranes were studied using the disk-like supports. The optimal conditions were then used with the tubular supports to produce the membranes for the PV tests. The experimental conditions are listed in Table 1.

Table 1. Experimental conditions used for synthesizing various membrane samples.

No.	Support	Seed	Precursor solution							Synthesis time (h)
			$Na_2WO_4 \cdot 2H_2O$	Acid	pH	Molar composition	$\frac{WO_3}{H_2O}$	$\frac{AcOH}{H_2O}$	$\frac{AcOH}{WO_3}$	
M1	ϕ30disk	-	1.15	HCl	2.0	$1NaO_2$:$1WO_3$: 1.58 HCl: $855H_2O$	0.0012	-	-	24
M2	ϕ30disk	-	1.15	AcOH	2.1	$1NaO_2$:$1WO_3$:175AcOH: $400H_2O$	0.0025	0.44	175	24
M3	ϕ30disk	+	1.15	AcOH	2.1	$1NaO_2$:$1WO_3$:175AcOH: $400H_2O$	0.0025	0.44	175	24
M4	ϕ30disk	+	1.15	AcOH	2.1	$1NaO_2$:$1WO_3$: 175AcOH: $400H_2O$	0.0025	0.44	175	12
M5	ϕ30disk	+	1.15	AcOH	2.1	$1NaO_2$:$1WO_3$: 175AcOH: $400H_2O$	0.0025	0.44	175	6
M6	ϕ30disk	+	1.15	AcOH	2.1	$1NaO_2$:$1WO_3$: 175AcOH: $400H_2O$	0.0025	0.44	175	3
M7	ϕ11disk	+	0.23	AcOH	2.0	$1NaO_2$:$1WO_3$:476AcOH:$3270H_2O$	0.0003	0.15	476	24
M8	ϕ11disk	+	0.46	AcOH	2.0	$1NaO_2$:$1WO_3$:313AcOH:$1400H_2O$	0.0007	0.22	313	24
M9	ϕ11disk	+	0.80	AcOH	2.0	$1NaO_2$:$1WO_3$:216AcOH: $690H_2O$	0.0015	0.31	216	24
M10	ϕ11disk	+	1.15	AcOH	2.1	$1NaO_2$:$1WO_3$:175AcOH: $400H_2O$	0.0025	0.44	175	24
M11	ϕ11disk	+	2.30	AcOH	2.2	$1NaO_2$:$1WO_3$: 88 AcOH: $201H_2O$	0.0050	0.44	88	24
M12	ϕ11disk	+	2.30	AcOH	2.2	$1NaO_2$:$1WO_3$: 88 AcOH: $201H_2O$	0.0050	0.44	88	24
M13	tube	+	1.15	AcOH	2.1	$1NaO_2$:$1WO_3$:175AcOH: $400H_2O$	0.0025	0.44	175	24
M14	tube	+	2.30	AcOH	2.2	$1NaO_2$:$1WO_3$: 88 AcOH: $201H_2O$	0.0050	0.44	88	24
M15	tube	+	2.30	AcOH	2.2	$1NaO_2$:$1WO_3$: 88 AcOH: $201H_2O$	0.0050	0.44	88	24
M16	tube	+	2.30	AcOH	2.2	$1NaO_2$:$1WO_3$: 88 AcOH: $201H_2O$	0.0050	0.44	88	24
M17	tube	+	2.30	AcOH	2.2	$1NaO_2$:$1WO_3$: 88 AcOH: $201H_2O$	0.0050	0.44	88	24

M18	tube	+	2.30	AcOH	2,2	1NaO_2:1WO_3: 88 AcOH: 201H_2O	0.0050	0.44	88	24

2.3. Characterization

The crystalline phases and degrees of crystal alignment of the membranes were characterized by X-ray diffraction (XRD) analysis (Rigaku Corporation, Ultima IV) performed using Cu-Kα radiation. The surfaces and cross-sections of the membranes were observed using a scanning electron microscopy (SEM) system (Hitachi High-Tech Corporation, S-4800). Elemental analysis was performed using energy-dispersive X-ray spectroscopy (EDX, Horiba, Ltd., E-Max). The hydrophilic-hydrophobic character was discussed from the viewpoint of contact angle. The contact angles of H_2O and AcOH were measured using a 2 μl droplet on the NP-h-WO_3 membrane formed on the disk-like support to consider the effect of hydrophilic-hydrophobic character on the H_2O/AcOH separation performances of the membrane.

2.4. Evaluation of separation performance

The H_2O/AcOH separation performances of the membranes were evaluated through PV tests. Figure 1 shows a schematic illustration of the apparatus used. One side of the test NP-h-WO_3 membrane was attached to a glass tube (outer diameter: 10 mm; inner diameter: 8 mm) while the other side was blocked with a dense alumina plate using a silicone resin. The membrane was then soaked in H_2O/AcOH mixtures heated to 353 K. The permeate side of the membrane was always kept at 0.3 ± 0.1 kPa using a vacuum controller. The permeate collected within the first hour was removed, and the performance of the membrane was evaluated using the permeate collected thereafter, which was fixed to 10 hours for H_2O/AcOH mixtures. The effect of permeate removed within the first hour was negligible for the H_2O/AcOH mixtures because it only accounted for less than 0.005% of the feed concentration. For the separation of H_2O/AcOH mixtures, the AcOH concentrations of the

feed and the permeate were determined using a reflectometer (Atago Co. Ltd., PAL-RI). The total flux (F), separation factor (a), and permeabilities of water (P_{H2O}) and AcOH (P_{AcOH}) were calculated using the following equations:

$$F = \frac{m}{A \times t} \quad (1)$$

$$\alpha = \frac{Y_{H_2O}/Y_{AcOH}}{X_{H_2O}/X_{AcOH}} \quad (2)$$

$$P_{H_2O} = \frac{(m/M_{H_2O}) \times Y_{H_2O}}{A \times (t/3600) \times \Delta p_{H_2O}} \quad (3)$$

$$P_{AcOH} = \frac{(m/M_{AcOH}) \times Y_{AcOH}}{A \times (t/3600) \times \Delta p_{AcOH}} \quad (4)$$

where X_{H2O}, X_{AcOH}, Y_{H2O}, and Y_{AcOH} denote the mass fractions of water and AcOH on the feed side and those on the permeate side, respectively. Further m is the total amount of the permeate (kg); A is the effective membrane area (m^2); t is the testing time (h); M_{H2O} and M_{AcOH} are the molecular weights of H_2O and AcOH, respectively; and Δp_{H2O} and Δp_{AcOH} are the partial pressure differences (Pa) of H_2O and AcOH across the membrane, respectively.

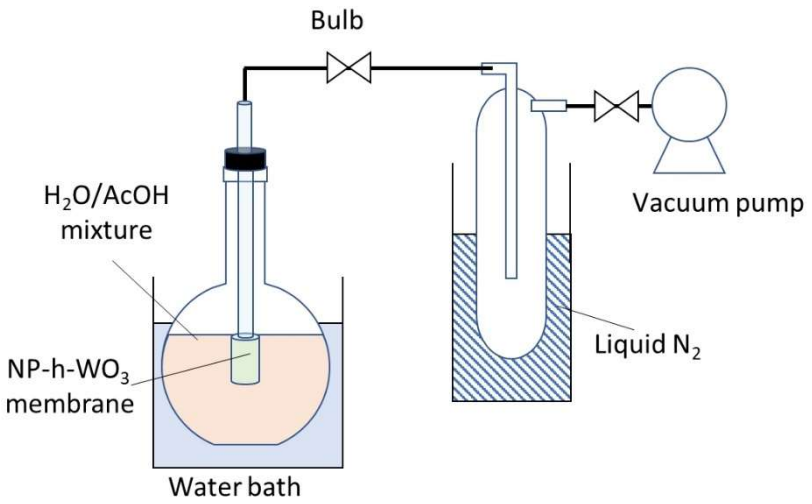

Figure 1. Schematic of apparatus used for PV tests.

2.5. Evaluation of single component permeation

The single component permeation properties of the membranes were evaluated through PV tests in a similar manner with the separation tests. The membrane was soaked in the pure solvents and the temperature was adjusted according to the solvent so that the pressure differences of the single component across the membrane were around 40 kPa. Again, the permeate collected within the first hour was removed, and the permeate was collected after another 1 hour. Permeabilities of single components (P_{Sx}) were calculated using the following equation:

$$P_{Sx} = \frac{(m_x/M_x)}{A\times(t/36\quad)\times\Delta p_x} \tag{5}$$

where x is the target component, m_x is the amount of the permeate of component x (kg); M_x is the molecular weights of component x; and Δp_x is the partial pressure differences (Pa) of component x across the membrane, respectively.

3. Results and discussion

3.1. Effects of addition of AcOH to precursor solution

Figure 2 show the XRD patterns and SEM images of the membranes synthesized at 453 K for 24 h using the precursor solutions containing HCl (M1) and AcOH (M2), respectively. The XRD patterns matched that of h-WO_3 (PDF card #01-075-2187), indicating that h-WO_3 was synthesized successfully from both precursor solutions. However, the two membranes showed obvious differences in their crystal alignments. The membrane synthesized from the precursor solution containing AcOH (M2) showed a significantly higher degree of c-plane alignment compared with that of the membrane formed using the solution containing HCl (M1). This is based on the fact that, in the former case, the reflection of the (001) plane was stronger compared with those of the (100) and (200) planes. This implies that AcOH results in greater crystal alignment along the c-plane of h-WO_3, which is advantageous, since the nanopores exist on the c-plane of h-WO_3. It can be seen from the

SEM images that the h-WO_3 crystals synthesized using the precursor solutions containing HCl exhibited a thin, whisker-like morphology while those synthesized from the precursor solutions containing AcOH exhibited a thicker, pillar-like morphology. Moreover, the thickness of the crystals synthesized using AcOH was approximately five times greater. Several researchers have reported that h-WO_3 crystallizes to exhibit an elongated whisker-like morphology along the c-axis direction [15,21,24]. Thus, the obtained results implied that the use of AcOH enhanced crystal growth along the c-plane. This correlates with the result that the intensity of the XRD peaks related to the c-plane was significantly higher. Miyamoto et al. [25] reported that AcOH acts as a structure-directing agent and exploited this fact to control the crystal alignment of UiO-66 films. In the present study as well, the AcOH molecules may have been adsorbed onto the nanopores of h-WO_3 and inhibited crystal growth along the c-axis. Based on these results, the precursor solution containing AcOH was used for the rest of the study.

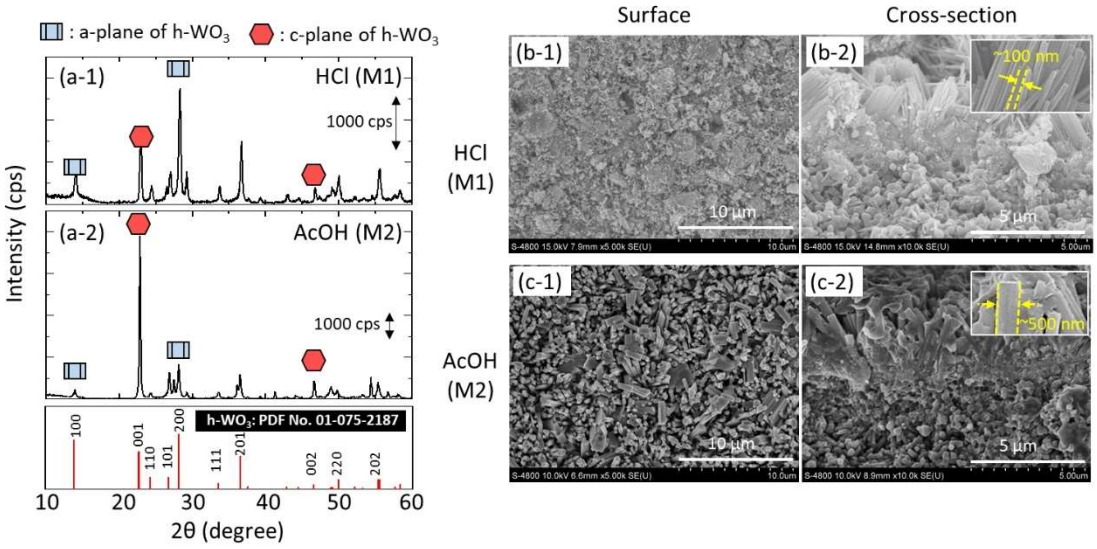

Figure 2. XRD patterns and SEM images of membranes prepared using (a-1, b-1, b-2) HCl and (a-2, c-1, c-2) AcOH.

3.2. Effects of preseeding of amorphous WO_3 on porous support

Figure 3 shows the XRD patterns and cross-sectional SEM images of the membranes synthesized at 453 K for 24 h with precursor solutions containing AcOH using ceramic supports without and with amorphous WO_3 seeds (M2 and M3, respectively). Amorphous WO_3 seeds with a diameter of approximately 300 nm were previously coated on the surface of the support (Fig. S1). The results of the XRD analysis showed that both conditions resulted in films with a high degree of c-plane alignment; however, the low intensity of the peaks related to the a-plane implied that the membrane synthesized on the preseeded support exhibited a slightly higher degree of alignment along the c-plane. The SEM images of the cross-sections of the membranes indicated that seeding increased the uniformity of the membrane thickness as well as the degree of c-plane alignment. Furthermore, seeding led to the densification of the membranes, as evidenced by the decrease in the size of the gaps observed between the NP-h-WO_3 crystals comprising the membranes. It has been reported that, during the synthesis of zeolite membranes, seeds can serve as nuclei and promote growth near the surface of the support [26, 27]. Thus, it is likely that the amorphous WO_3 seeds similarly promoted the crystallization of NP-h-WO_3 near the surface of the ceramic support. Hence, seeding was adopted for the rest of the experiments.

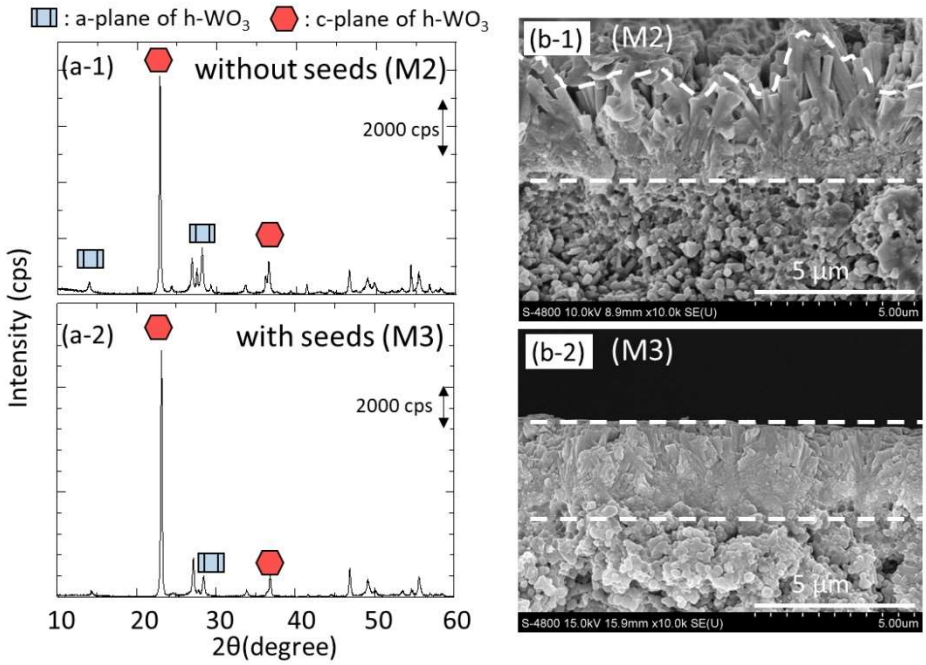

Figure 3. XRD patterns and cross-sectional SEM images of membranes prepared using supports (a-1, b-1) without and (a-2, b-2) with amorphous WO_3 seeds.

3.3. Effects of synthesis time

The XRD patterns and cross-sectional SEM images of the membranes synthesized at 453 K for 3, 6, 12, and 24 h using precursor solutions containing AcOH and seeded supports are shown in Fig. 4 and 5, respectively. In the case of the membrane with a synthesis time of 3 h (M6), high-intensity peaks related to the support were observed while no peak related to h-WO_3 could be distinguished. For synthesis times of 6 h and greater (M5, M4, and M3), distinct peaks related to h-WO_3 were seen while those related to the support became weak, meaning that the coverage of the NP-h-WO_3 crystals on the support increased. Based on the intensities of the (001) and (200) peaks, which corresponded to the c- and a-planes of h-WO_3, respectively, it can be concluded that the extent of crystal alignment along the c-plane was enhanced with an increase in the synthesis time. These results are in keeping with the SEM observations. Only a few NP-h-WO_3 crystals were observed after 3 h, while pillar-like h-

WO_3 crystals covered the entire support after 6 h. For longer synthesis times, the membranes were denser, as confirmed by the decrease in the gaps between the pillar-like crystals (Fig. 5 (b-3), (c-3), and (d-3)). The enhancement in the degree of crystal alignment was likely due to the decrease in the reflections from the tilted h-WO_3 crystals.

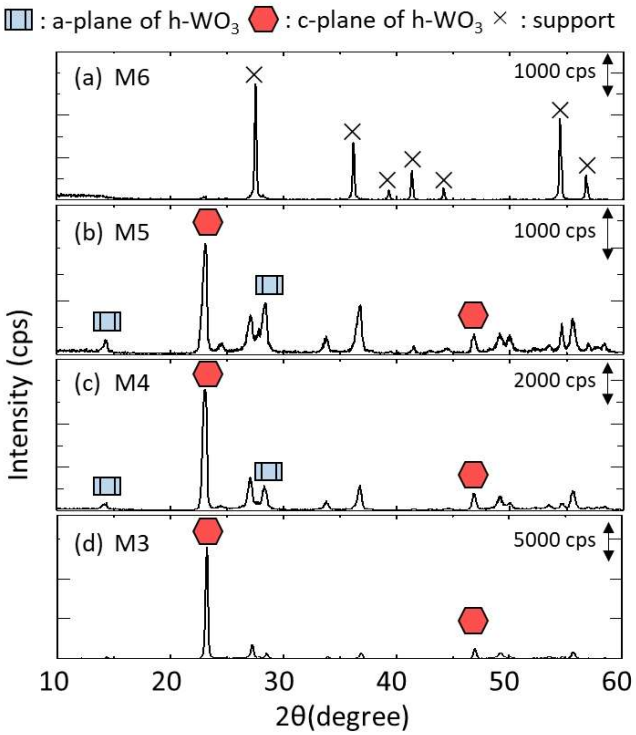

Figure 4. XRD patterns of membranes synthesized for (a) 3, (b) 6, (c) 12, and (d) 24 h.

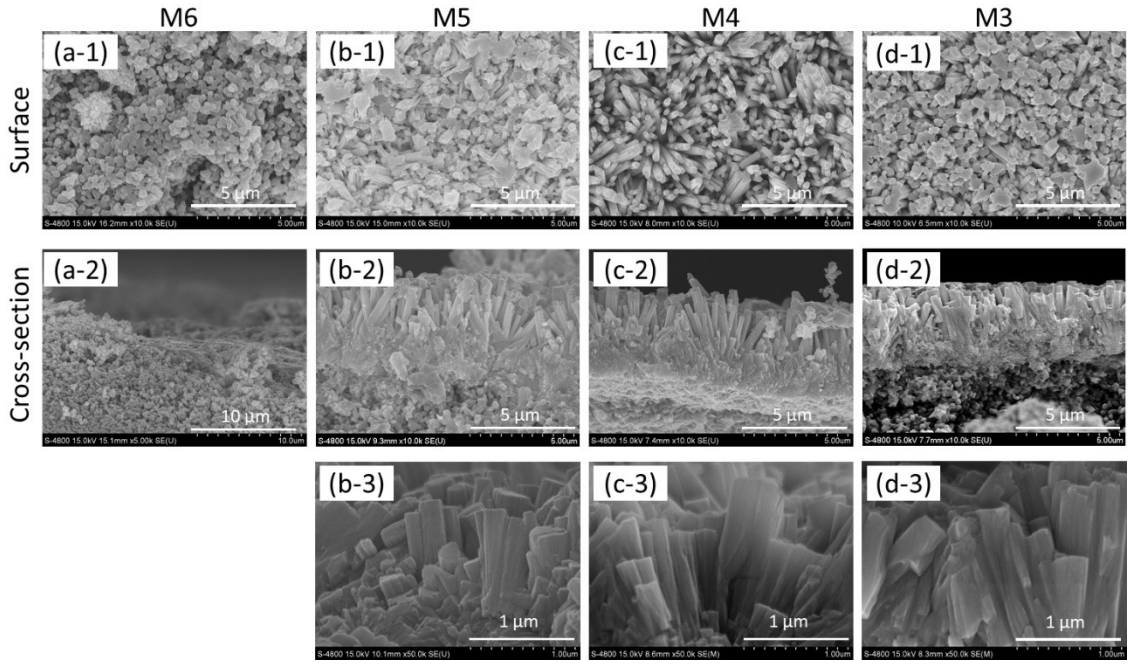

Figure 5. Surface (-1) and cross-sectional (-2) SEM images of membranes synthesized for (a) 3, (b) 6, (c) 12, and (d) 24 h. High magnification images of (b-2), (c-2), and (d-2) are shown in (b-3), (c-3), and (d-3), respectively.

The relationship between the synthesis time and membrane thickness is shown in Fig. 6. The membrane thickness increased dramatically for a synthesis time of 6 h. This means that the induction period for membrane synthesis should be 3–6 h. For synthesis periods longer than 6 h, the membrane thickness increased only slightly. This may be because the crystal growth primarily occurred within the gaps between the crystals, leading to the densification of the membrane. Thus, a long crystallization time may be essential for obtaining high-quality membranes.

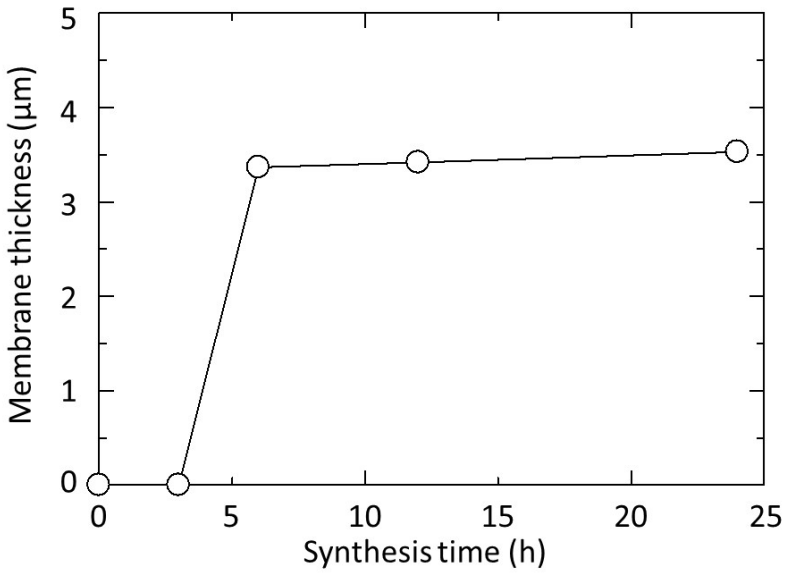

Figure 6. Relationship between synthesis time and membrane thickness.

3.4. Effects of Na_2WO_4 content of precursor solution

Figure 7 shows the XRD patterns of the NP-h-WO_3 membranes synthesized at 453 K for 24 h using seeded supports and precursor solutions containing AcOH with different amounts of $Na_2WO_4{\cdot}2H_2O$ (M7 to M11). When the amount of $Na_2WO_4{\cdot}2H_2O$ was 0.23 g, WO_3 crystallized in the orthorhombic phase (o-WO_3) was observed. Further, NP-h-WO_3 membranes could be synthesized using the precursor solutions with more than 0.46 g of $Na_2WO_4{\cdot}2H_2O$. The membranes synthesized using the solution with 0.46 g of $Na_2WO_4{\cdot}2H_2O$ showed higher-intensity reflections related to the a-plane as compared with those related to the c-plane. On the other hand, the membrane synthesized using the solution with more than 0.80 g of $Na_2WO_4{\cdot}2H_2O$ showed higher-intensity peaks related to the c-plane as compared with those of the a-plane. The intensity of the c-plane peaks increased gradually with the increase in the $Na_2WO_4{\cdot}2H_2O$ content, such that all the crystals were almost completely aligned with the c-plane when the $Na_2WO_4{\cdot}2H_2O$ content was 2.30 g. This result indicates that a high Na_2WO_4 content is essential for ensuring that the crystals are aligned along the c-plane.

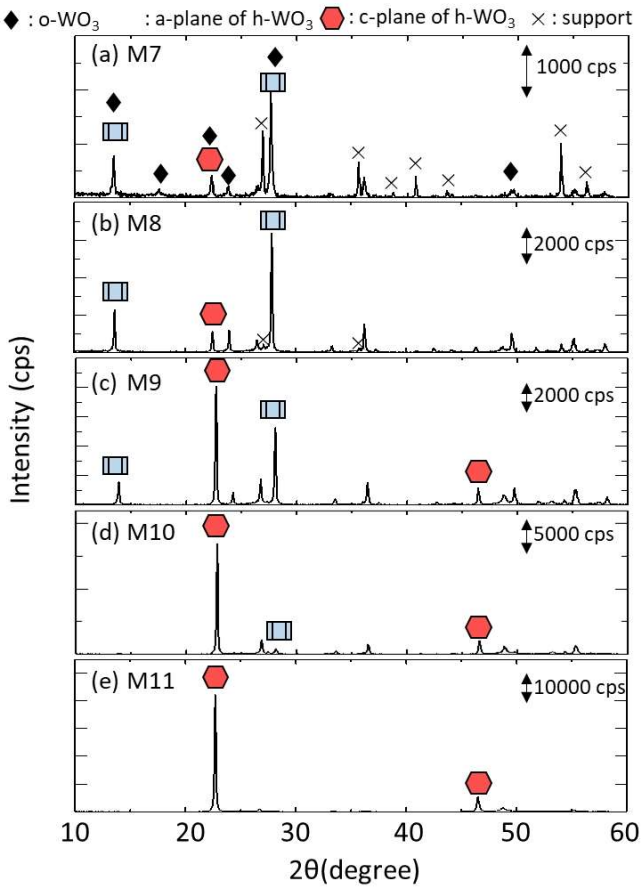

Figure 7. XRD patterns of membranes synthesized using precursor solutions with (a) 0.23, (b) 0.46, (c) 0.80, (d) 1.15, and (e) 2.30 g of $Na_2WO_4 \cdot 2H_2O$.

Figure 8 shows SEM images of the surface and cross-sections of the NP-h-WO_3 membranes synthesized at 453 K for 24 h using seeded supports and precursor solutions containing AcOH with different amounts of $Na_2WO_4 \cdot 2H_2O$. The extent of coverage of the WO_3 crystals was extremely low when the solution with only 0.23 g of $Na_2WO_4 \cdot 2H_2O$ was used; this explains why peaks related to the support were observed in the corresponding XRD pattern. When the solution with 0.46 g of $Na_2WO_4 \cdot 2H_2O$ was used, the coverage increased drastically. However, the c-axes of the pillar-like h-WO_3 bundles were aligned in random directions, meaning that they were not aligned along the c-plane. Further, the surface of the

support was partially uncovered. When the amount of $Na_2WO_4 \cdot 2H_2O$ was increased to 0.80 g, the morphology of the membrane surface changed from that observed in the case of the lower Na_2WO_4 concentrations. A large number of pillar-like crystals growing perpendicular to the support surface were observed, implying that their c-axes were perpendicular to the support surface. This conclusion is supported by the results of the XRD analysis, which showed that the intensity of the c-plane peaks became stronger than those of the a-plane peaks, in contrast to the case for the lower Na_2WO_4 concentrations. Further increases in the $Na_2WO_4 \cdot 2H_2O$ concentration to 1.15 and 2.30 g resulted in pillar-like crystals that were almost perfectly aligned perpendicular to the support surface. This led to denser membranes. The interface of the NP-h-WO_3 membrane and the support could be distinguished clearly in the elemental maps and line profile obtained using EDX (Fig. S2), meaning that the h-WO_3 crystals did not penetrate deep within the support. The thickness of the membrane synthesized using the precursor solution with 2.30 g of $Na_2WO_4 \cdot 2H_2O$ was approximately 8.5 μm.

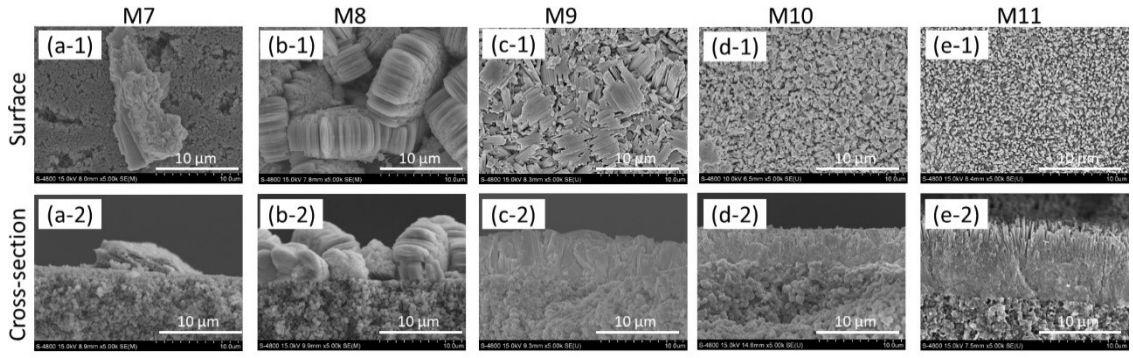

Figure 8. Surface and cross-sectional SEM images of membranes synthesized using precursor solutions with (a-1, a-2) 0.23, (b-1, b-2) 0.46, (c-1, c-2) 0.80, (d-1, d-2), 1.15, and (e-1, e-2) 2.30 g of $Na_2WO_4 \cdot 2H_2O$.

3.5. Synthesis of NP-h-WO_3 membrane on tubular support

Based on the experimental results obtained using the disk-like supports, it was determined that the use of a seeded support and a precursor solution containing AcOH and Na_2WO_4 in a high concentration were the optimal conditions for obtaining high-quality membranes. Thus, the conditions for M11; which is synthesized at 453 K for 24 h using seeded supports and precursor solutions containing AcOH and $Na_2WO_4{\cdot}2H_2O$ of 2.30 g, were adopted in the case of the tubular support as well. The XRD pattern and SEM images of the membrane grown on the tubular support is shown in Fig. 9. The membrane synthesized on the tubular support exhibited higher-intensity c-plane peaks as compared with those related to the a-plane, meaning that the crystals were aligned along the c-plane. The remaining reflections related to the a-plane of h-WO_3 can be attributed to the attachment of the h-WO_3 crystals nucleated in the bulk solution during the synthesis process. The SEM image of the membrane surface (Fig. 9(b)) shows the presence of bulky bundles of pillar-like crystals aligned parallel to the support surface. Meanwhile, pillar-like crystals perpendicular to the support surface were observed beneath these bundles, as shown in Fig. 9(c-2). The prevention of the nucleation of crystals and their attachment from the bulk solution is thus essential when using tubular supports. The membrane growth was expected to be similar to that observed in the disk-like supports, except for the attachment of the bundle like crystals, because it showed a similar membrane thickness of around 8 μm. Finally, five membranes (M14 to M18) were synthesized under the same conditions to confirm the reproducibility of the process. The conditions of using a precursor solution with less $Na_2WO_4{\cdot}2H_2O$ (1.15 g, M10) was also prepared for comparison.

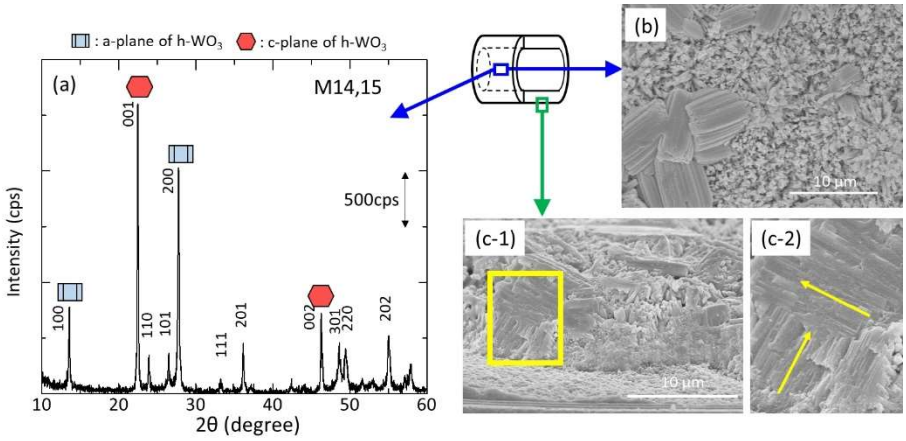

Figure 9. XRD patterns and SEM images of membranes prepared on tubular support. (a) XRD pattern and (b) and (c) SEM image of surface and cross-section of tubular membrane. (c-2) is high-magnification image of area within yellow box in (c-1).

3.6. Evaluation of separation performance

The PV performances of the NP-h-WO_3 membranes prepared on the tubular supports were investigated using a binary H_2O/AcOH mixture (10/90 (w/w)) with a pH below 0. The results are listed in Table 2. The four NP-h-WO_3 membranes prepared under the optimum condition (M14, M15, M16, M17); which is synthesized at 453 K for 24 h using seeded supports and precursor solutions containing AcOH and $Na_2WO_4{\cdot}2H_2O$ of 2.30 g, showed similar F and α values. The percentage of variation in their performance was smaller than that of a previous study dealing the reproducibility of mordenite membranes [28], meaning that the membrane synthesis process is a reproducible one to some extent. Meanwhile, the membrane prepared with less $Na_2WO_4{\cdot}2H_2O$ of 1.15 g (M13) did not show complete coverage, implying a high $Na_2WO_4{\cdot}2H_2O$ amount was effective to promote the densification of the membrane. Further, both NP-h-WO_3 membranes exhibited water-selective permeability, as expected from the sizes of the H_2O and AcOH molecules and the pore size of h-WO_3. The maximum selectivity with respect to permeability (P_{H2O}/P_{AcOH}) exceeded 35, implying that the nanopores of h-WO_3 exhibited a molecular sieving effect. This will be

discussed in detail from the results of contact angle measurements and the single component permeation afterwards. The maximum performance, that is, the highest P_{H2O} and α values, exhibited by the NP-h-WO_3 membranes were 4.94×10^{-8} mol/(m^2・s・Pa) and 42.7, respectively. Further improvements such as preventing the attachment of bundle crystals on the membrane surface are expected to increase the performance of the membranes.

Table 2. Separation performance of synthesized NP-h-WO_3 membranes for binary H_2O/AcOH mixture (10/90 (w/w)).

No.	F (kg/(m^2·h))	P_{H2O} (mol/(m^2·s·Pa))	P_{AcOH} (mol/(m^2·s·Pa))	P_{H2O}/P_{AcOH} (-)	α (-)
M14	0.0350	4.94×10^{-8}	2.50×10^{-9}	19.8	23.3
M15	0.0312	5.05×10^{-8}	1.39×10^{-9}	36.4	42.6
M16	0.0275	4.07×10^{-8}	1.57×10^{-9}	25.9	29.7
M17	0.0225	3.11×10^{-8}	1.60×10^{-9}	19.5	23.0

Furthermore, the effect of feed concentration was considered using membrane M16. Table 3 shows the result of H_2O/AcOH separation for binary H_2O/AcOH mixture of 10/90 (w/w), 30/70 (w/w), and 50/50 (w/w). Both P_{H2O} and P_{AcOH} increased along with the decrease in AcOH concentration, while the separation factor α increased by decreasing the AcOH concentration of the feed. The membrane exhibited a maximum separation factor of α= 41.9 of separation factor when using a binary H_2O/AcOH mixture of 50/50 (w/w). The increase in separation factor may be explained by the increase in partial pressure of H_2O and decrease in that of AcOH.

Table 3. Effect of feed concentration on separation performance of NP-h-WO_3 membranes.

No.	H_2O/AcOH (w/w)	pH	F (kg/(m^2·h))	P_{H2O} (mol/(m^2·s·Pa))	P_{AcOH} (mol/(m^2·s·Pa))	P_{H2O}/P_{AcOH} (-)	α (-)
M16	10/90	< 0	0.0275	4.07×10^{-8}	1.57×10^{-9}	25.9	29.7
M16	30/70	0.5	0.0942	5.34×10^{-8}	2.73×10^{-9}	19.6	41.9
M16	50/50	1.1	0.1607	6.79×10^{-8}	4.49×10^{-9}	15.1	42.0

3.7. Evaluation of acidic resistance

Figure 10 shows separation performance of membrane M17 after long-term soaking in a binary H_2O/AcOH mixture of 10/90 (w/w) with a pH below 0. After conducting the first separation test for 10 hours, the membrane was continuously soaked and stored in the binary H_2O/AcOH mixture for 3 nights. Then, the second separation test was conducted again for 10 hours and the membrane performance was compared with that of the first test. The membrane exhibited permeance change of less than 5% and a constant separation factor of approximately 23 regardless of the soaking time, indicating that the membrane was not deteriorated by the low pH of below 0 even after approximately 80 hours. The slight change in permeance may be due to the slight fluctuation of the water bath temperature during the 10-hour run. The acid stability was further considered by soaking a NP-h-WO_3 membrane prepared on a disk-like support under the same synthesis condition in a binary H_2O/AcOH mixture of 10/90 (w/w) with a pH below 0 at 353 K for 120 hours. The XRD patterns and cross-sectional SEM images showed no sign of deterioration even after soaking at 353 K for 120 hours (Fig. S3). Moreover, no weight change was observed before and after soaking (Table S1), which well corresponds to expectations from the potential-pH diagram recalculated for 353 K from reference 29 indicating WO_3 is stable below pH<4. These prove the high acidic resistance of the newly developed NP-h-WO_3 membrane. This high acid resistance of h-WO_3 membranes show great promise in the separation of acidic mixtures such as H_2O/AcOH mixtures.

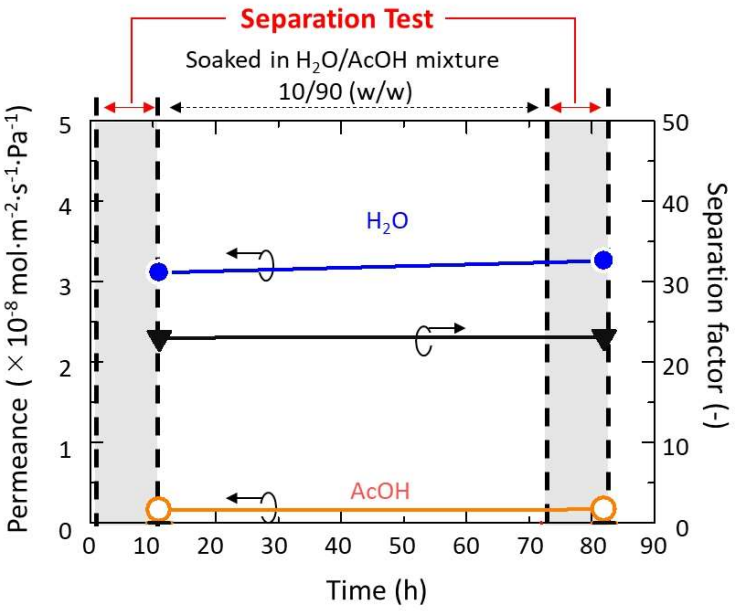

Figure 10. Separation performance of NP-h-WO_3 membrane after long-term soaking in a binary H_2O/AcOH mixture of 10/90 (w/w) with a pH below 0.

3.8. Separation mechanism of the NP-h-WO_3 membrane

From the aforementioned results, the dehydration ability of the novel NP-h-WO_3 membranes have been confirmed. However, it is not clear whether this separation is based on the hydrophilicity of the membrane or the molecular sieving property of the NP-h-WO_3. Thus, contact angle measurements and single component permeation tests were conducted to evaluate the hydrophilic-hydrophobic character and molecular sieving ability of NP-h-WO_3 membranes.

Figure 11 shows the contact angle measurement for H_2O and AcOH droplets on NP-h-WO_3 membrane synthesized at 453 K for 24 h using precursor solutions containing AcOH and $Na_2WO_4 \cdot 2H_2O$ of 2.30 g on the seeded disk-like support (M12). The membrane was buff-polished with alumina particles of 0.05 μm before the measurement to obtain a smooth surface, as shown in Fig. 11 (a). Contact angle on the NP-h-WO_3 membrane was 74 degrees for H_2O (Fig. 11 (b-1)) while it was 18 degrees for AcOH (Fig. 11 (b-2)). This means that the wettability of AcOH was better than H_2O against the NP-h-WO_3 membrane. This implies that the

hydrophilicity was not the cause for separation of H_2O/AcOH mixtures because the less wettable H_2O selectively permeated in this study.

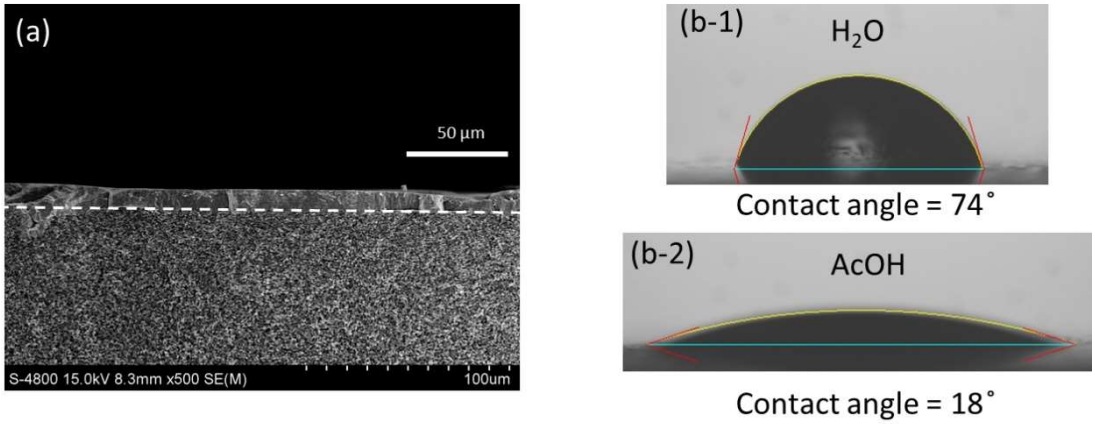

Figure 11. Cross-sectional image of flat NP-h-WO_3 membrane on disk-like support after buff polish (a), and contact angle for droplets of H_2O (b-1) and AcOH (b-2) on the NP-h-WO_3 membrane.

Figure 12 shows the single component permeance of various solvents across the NP-h-WO_3 membrane (M18), synthesized at 453 K for 24 h using seeded tubular support and a precursor solution containing AcOH and $Na_2WO_4{\cdot}2H_2O$ of 2.30 g, against the molecular size (i.e. kinetic diameter). The permeance of H_2O was an order of magnitude higher than those of MeOH, EtOH, AcOH and Actn, indicating there is an obvious cut off in the size range between the H_2O molecule and MeOH molecule. This can be well explained by the size of the nanopores of NP-h-WO_3, which is reported to be 0.367nm [17] The kinetic diameter of MeOH, EtOH, AcOH, Actn are 0.380 nm, 0.430 nm, 0.436 nm and 0.469 nm, respectively [30]. Because the kinetic diameter of the molecules of the tested organic solvents were all larger than the diameter of the nanopores of NP-h-WO_3 while the H_2O molecules were smaller, only the H_2O must have been able to permeate through the nanopores of NP-h-WO_3. From these results, the separation

of H_2O/AcOH mixtures were anticipated to be based on the molecular sieving effect and not the hydrophilicity of the NP-h-WO_3 membranes.

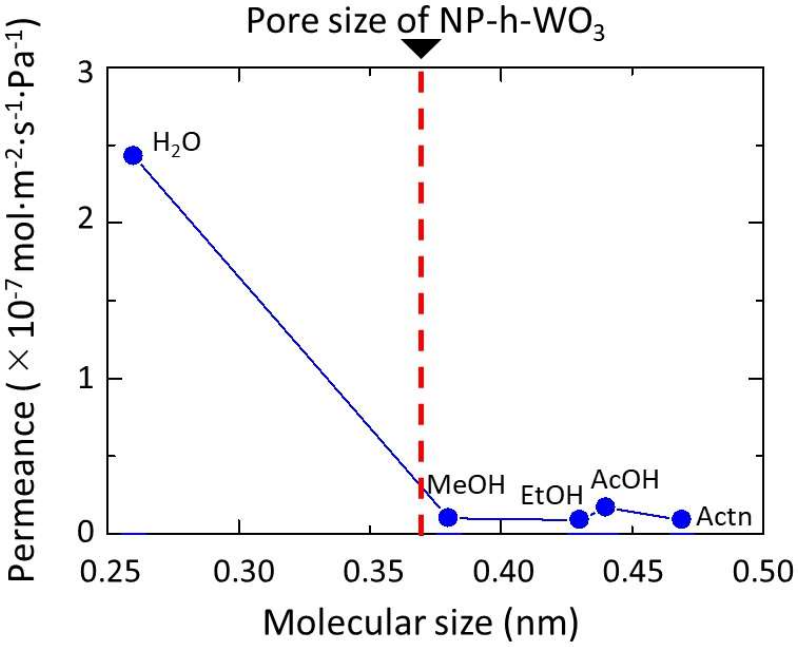

Figure 12. Relation between single component permeance of various solvents and their molecular size (pressure difference along the membrane: approx. 40 kPa). The red broken line indicates the size of nanopores of NP-h-WO_3 reported in previous literature [17].

4. Conclusions

In this study, we synthesized, for the first time, c-plane-aligned NP-h-WO_3 membranes that can separate H_2O/AcOH mixtures. The presence of AcOH and the addition of Na_2WO_4 in high concentrations to the synthesis solution were found to be essential for both crystal growth and alignment along the c-plane. Moreover, precoating the support surface with amorphous WO_3 seeds was effective in producing dense membranes with a homogeneous thickness. Thus, dense, c-plane-aligned membranes could be obtained by the hydrothermal treatment using a preseeded support in a precursor solution of Na_2O/WO_3/AcOH/H_2O (1:1:88:201) at 180 °C for 24 h. The fabricated membranes exhibited

a maximum separation factor of 42.6 and P_{H2O} of 4.94×10^{-8} mol/(m^2・s・Pa) during PV tests performed using 10/90 (w/w) H_2O/AcOH mixtures at 80 °C. The contact angle measurements and single component permeation results implied that the separation was based on the molecular sieving effect and not the hydrophilicity of the NP-h-WO_3 membrane. Considering the high acidic resistance of WO_3, these NP-h-WO_3 membranes have significant potential for use in the separation of H_2O/AcOH mixtures.

Acknowledgments

This work was mainly supported by a Grant-in-Aid for Scientific Research (KAKENHI) [grant number JP19K15336] from the Japan Society for the Promotion of Science and partially supported by the Project of Creation of Life Innovation Materials for Interdisciplinary and International Researcher Development of the Ministry of Education, Culture, Sports, Science and Technology, Japan and a research grant from the Kyosho Hatta Foundation. In addition, we would like to thank Editage (http://www.editage.com) for editing and reviewing this manuscript for English language.

References

1. K. Ueno, H. Negishi, M. Miyamoto, S. Uemiya, Y. Oumi, Effect of Si/Al ratio and amount of deposited MFI-type seed crystals on the separation performance of silicalite-1 membranes for ethanol/water mixtures in the presence of succinic acid, Microporous Mesoporous Mater., 267 (2018) 1-8.
2. B. Huang, Q. Liu, J. Caro, A. Huang, Iso-butanol dehydration by pervaporation using zeolite LTA membranes prepared on 3-aminopropyltriethoxysilane-modified alumina tubes, J. Memb. Sci., 455 (2014) 200-206.

3. J. Zhang, Y. He, Y. Wang, J. Mao, X. Cui, Synthesis of a self-supporting faujasite zeolite membrane using geopolymer gel for separation of alcohol/water mixture, Mater. Lett., 116 (2014) 167-170.
4. R. Zhou, Z. Hu, N. Hu, L. Duan, X. Chen, H. Kita, Preparation and microstructural analysis of high-performance mordenite membranes in fluoride media, Mesoporous Mater., 156 (2012) 166-170.
5. C. Xu, X. Lu, Z. Wang, Effects of sodium ions on the separation performance of pure-silica MFI zeolite membranes, J. Memb. Sci., 524 (2017) 124-131.
6. X. Li, H. Kita, H. Zhu, Z. Zhang, K. Tanaka, K. Okamoto, Influence of the hydrothermal synthetic parameters on the pervaporative separation performances of CHA-type zeolite membranes, Mesoporous Mater., 143 (2011) 270-276.
7. M. Zhu, S. Xia, X. Hua, Z. Feng, N. Hu, F. Zhang, I. Kumakiri, Z. Lu, X. Chen, H. Kita, Rapid preparation of acid-stable and high dehydration performance mordenite membranes, Ind. Eng. Chem. Res., 53 (2014) 19168−19174.
8. Y. Hasegawa, C. Abe, M. Nishioka, K. Sato, T. Nagase, T. Hanaoka, Formation of high flux CHA-type zeolite membranes and their application to the dehydration of alcohol solutions, J. Memb. Sci., 364 (2010) 318-324.
9. Z. Lai, G. Bonilla, I. Diaz, J. G. Nery, K. Sujaoti, M. A. Amat, E. Kokkoli, O. Terasaki, R. W. Thompson, M. Tsapatsis, D. G. Vlachos, Microstructural optimization of a zeolite membrane for organic vapor separation, Science, 300 (2003) 456-460.
10. K. Ueno, H. Negishi, M. Miyamoto, S. Uemiya, Y. Oumi, Effect of deposition seed crystal amount on the α-Al_2O_3 support and separation performance of silicate-1 membranes for acetic acid/water mixtures, Sep. Purif. Technol., 174 (2017)57-65.

11. Y. Hasegawa, Development of acid-tolerant zeolite membrane and application to chemical reactions, Membrane, 36 (2011) 84-90.

12. X. Li, H. Kita, H. Zhu, Z. Zhang, K. Tanaka, Synthesis of long-term acid-stable zeolite membranes and their potential application to esterification reactions, J. Membr. Sci., 339 (2009) 224-232.

13. Y. M. Shirke, S. P. Mukherjee, Selective synthesis of WO_3 and $W_{18}O_{49}$ nanostructures: ligand-free pH-dependent morphology-controlled self-assembly of hierarchical architectures from 1D nanostructure and sunlight-driven photocatalytic degradation, CrystEngComm, 19 (2017) 2096-2105.

14. H. Zheng, J. Z. Ou, M. S. Strano, R. B. Kaner, A. Mitchell, K. Kalantarzadeh, Nanostructured tungsten oxide – properties, synthesis, and applications, Adv. Funct. Mater., 21 (2011) 2175-2196.

15. B. Miao, W. Zeng, S. Hussain, Q. Mei, S. Xu, H. Zhang, Y. Li, T. Li, Large scale hydrothermal synthesis of monodisperse hexagonal WO_3 nanowire and the growth mechanism, Mater. Lett., 15 (2015) 12-15.

16. F. Zheng, M. Guo, M. Zhang, Hydrothermal preparation and optical properties of orientation-controlled WO_3 nanorod arrays on ITO substrates, CrystEngComm, 15 (2013) 277-284.

17. W. Sun, M. T. Yeung, A. T. Lech, C. W. Lin, C. Lee, T. Li, X. Duan, J. Zhou, R. B. Kaner, High surface area tunnels in hexagonal WO_3, Nano Lett., 15 (2015) 4834-4838.

18. Y. Zhang, X. Qiu, Z. Hong, P. Du, Q. Song, X. Gu, All-silica DD3R zeolite membrane with hydrophilic-functionalized surface for efficient and highly-stable pervaporation dehydration of acetic acid, J. Membr. Sci., 581 (2019) 236-242.

19. M. I. Nave, K. G. Kornev, Complexity of products of tungsten corrosion: comparison of the 3D Pourbaix diagrams with the experimental data, Metall. Mater. Trans. A, 48 (2017) 1414-1424.

20. Z. Jiao, J. Wang, L. Ke, X. W. Sun, H. V. Demir, Morphology-tailored synthesis of tungsten trioxide (hydrate) thin films and their photocatalytic properties, ACS Appl. Mater. Interfaces, 3 (2011) 229-236.

21. M. Takacs, C. Ducso, A. E. Pap, Fine-tuning of gas sensitivity by modification of nano-crystalline WO_3 layer morphology, Sens. Actuators B Chem., 221 (2015) 281-289.

22. J. Wang, W. Khoo, P. S. Lee, J. Ma, Synthesis, Assembly, and electrochromic properties of uniform crystalline WO_3 nanorods, J. Phys. Chem. C, 112 (2008) 14306-14312.

23. H. Kunishi, T. Hagio, Y. Kamimoto, R. Ichino, Morphological control of tungsten oxide by organic addition, Abstract book of 29th Annual Meeting of MRS-Japan 2019, November 28 (2019) R-P28-025.

24. N. M. Shinde, A. D. Jagadale, V. S. Kumbhar, T. R. Rana, J. Kim, C. D. Lokhande, Wet chemical synthesis of WO_3 thin films for supercapacitor application, Korean J. Chem. Eng., 32 (2015) 974-979.

25. M. Miyamoto, S. Kohmura, H. Iwatsuka, Y. Oumi, S. Uemiya, In situ solvothermal growth of highly oriented Zr-based metal organic framework UiO-66 film with monocrystalline layer, CrystEngComm, 17 (2015) 3422-3425.

26. G. Li, E. Kikuchi, M. Matsukata, Separation of water–acetic acid mixtures by pervaporation using a thin mordenite membrane, Sep. Purif. Technol., 32 (2003) 199-206.

27. S. Basak, D. Kundu, M. K. Naskar, Low temperature synthesis of NaA zeolite membranes: The effect of primary and secondary crystallizations, Ceram. Int., 40 (2014) 12923-12930.

28. Y. Li, M. Zhu, N. Hu, F. Zhang, T. Wu, X. Chen, and H. Kita, Scale-up of high performance mordenite membranes for dehydration of water-acetic acid mixtures, J. Memb. Sci.,564 (2018) 174-183

29. M. Pourbaix, Atlas of Electrochemical Equilibria (translated from the French by James. A. Franklin), first ed., Pergamon Press/Cebelcor, Oxford/Brussels, 1966.

30. T.L. Rocca, E. Carretier, D. Dhaler, E. Louradour, T. Truong and P. Moulin, Purification of Pharmaceutical Solvents by Pervaporation through Hybrid Silica Membranes, Membranes, 9 (2019) 76-92.